ELSEVIER

Journal of Nuclear Materials 266–296 (1999) 911–916

journal of nuclear materials

# Dependence of the L–H transition on separatrix-wall gaps on TdeV

G.W. Pacher *, R. Decoste, Y. Demers, A. Cote, J.-L. Lachambre, C. Boucher, C. Cote, J.-L. Gauvreau, D. Lafrance, D. Pinsonneault, B. Quirion, N. Richard, M. St.-Onge, and the TdeV Team

*Centre Canadien Fusion Magnétique (CCFM), 1804 boulevard Lionel-Boulet, Varennes, Que., Canada, J3X 1S1*

**Abstract**

Steady-state H-modes have been obtained on TdeV both with ECRH and Lower Hybrid heating. Power thresholds are comparable with those predicted by the ITER scaling laws. A very pronounced threshold in edge density is observed, below which no L–H transitions occur. H–L transitions occur at significantly lower values of edge density. When the edge density exceeds the threshold, H-modes are produced both with an outboard limiter and with the divertor baffle within one density scrape-off layer of the separatrix. In the former case, confinement was degraded, in the latter, it was improved. 

*Keywords:* H-mode; Tokamak de Varennes; ELM

## 1. Introduction

Well-controlled stationary H-modes have been obtained on the TdeV tokamak ($R \sim 0.83$ m, $a \sim 0.22$ m, $\kappa \sim 1.1$) with ECRH heating of ~0.5 MW. With the power presently available, these H-modes remain in the type III ELM regime [1]. The effect of varying the distances between the plasma and various structures is investigated. We report on the L–H transition as these distances are varied.

## 2. Characteristics of the experiments

Most of the experiments reported here were carried out with ECRH heating and with the $\nabla B$ drift towards the divertor (favorable for H-mode). ECRH power was launched at 110 GHz, such that it was deposited at the second harmonic at approximately 5 cm vertically from the plasma centre. The magnetic field was therefore kept constant at ~2 T on axis. Line-average densities were limited to below $\sim 6 \times 10^{19}$ m$^3$ because at higher densities, refraction and cut-off limit the absorption in the central region of the plasma.

The ECRH power applied was in the range of 200–500 kW. Ohmic heating in the absence of ECRH was ~230 kW, dropping to ~100 kW at the highest ECRH power levels applied. The total input power thus varied by approximately a factor of two. H-modes were also obtained with Lower Hybrid heating alone.

The TdeV tokamak systems are sufficiently flexible to allow independent variation of outboard (inactive LHCD antenna) and lower (inactive divertor entrance baffle) plasma–wall separations, as well as of the separatrix–baffle distance of the upper active divertor. These variations can be performed with only minor effects on plasma shape and safety factor, while maintaining identical divertor strike points and pumping geometries. Fig. 1 illustrates the basic geometry of TdeV, and shows the extremes of the gap variation performed. The separatrix–baffle distance was varied between the normal geometry A (4.8 cm) and geometry B (~2 cm). The (inactive) Lower Hybrid antenna was advanced (detail C) to within 2 cm (1.1 cm according to

* Corresponding author. Tel.: +1-514 652 8882; fax: +1-514 652 8625; e-mail: pachert@ccfm.ireq.ca.

0022-3115/99/$ – see front matter 
PII: S0022-3115(98)00848-4

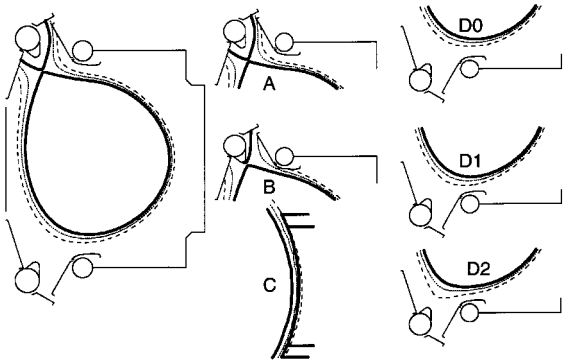


Fig. 1. Illustration of the magnetic geometry of TdeV including first-wall surfaces and illustrating the extrema investigated. Details A and B represent the normal and minimum separatrix–baffle gap, detail C the minimum outboard (OB) clearance, details D0 and D1 the normal and minimum lower clearance. Detail D2 is the higher bottom triangularity case. Flux is plotted as 5% contours.

magnetic reconstruction, ~2 cm when plasma centre is determined from interferometric measurements). The distance between the separatrix and the closest surface on the bottom of the machine was varied from 6.1 cm (D0) to 4.8 cm (D2), and was accompanied by a change in the lower triangularity of the 95% flux surface from 0.1 to 0.2. As discussed below, one density scrape-off layer is about 2 cm or 10% of poloidal flux.

The main diagnostic for density measurements is a 9-channel submillimeter interferometer. Eight channels are used for the reconstruction of the density profile. The reconstruction employs knowledge of the normal density gradient at the edge, obtained from reflectometer measurements, and allows a good estimate of the density at the separatrix [2].

The plasma density is controlled by gas fuelling, mainly in the plasma chamber, and by divertor pumping with a pumping speed of ~5 $m^3$/s. So as to obtain steady-state H-modes in view of the density modifications with heating power described in the preceding paragraph, one channel of the interferometer was used as a control signal, with an impact parameter of ~0.6 of the plasma minor radius.

## 3. Edge density dependence of L–H transition

A strong dependence of the H-mode transition on the separatrix density was observed. This behaviour, which is illustrated for one discharge on Fig. 2(a), is typical of all H-mode discharges on TdeV. The input power throughout is constant. Repetitive L–H transitions during this shot occurred at precisely the same value of separatrix density, $1.5 \times 10^{19}$ $m^{-3}$. The back transitions were all obtained at a lower value, $1.3 \times 10^{19}$ $m^{-3}$. During the H-mode, an increase of the type III ELM frequency with decreasing separatrix density is clearly observed, indicating that the power threshold is ap-

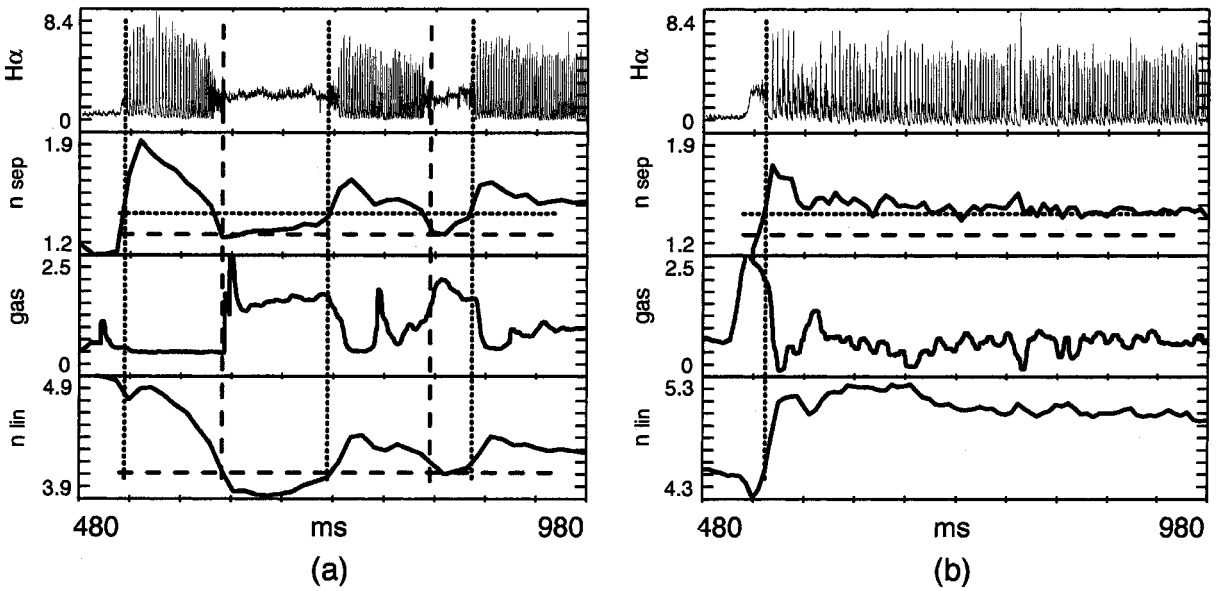


Fig. 2. Hα emission ($10^{19}$ photons/$m^2$/s), separatrix density, gas input rate (Pa-$m^3$/s), and line-average density plotted against time. Densities in ($10^{19}$ $m^{-3}$). (a) Repetitive H-modes, where the dotted lines indicate the separatrix density for L–H transition and the dashed lines that for H–L transition; (b) steady-state (500 ms) H-mode with threshold separatrix densities from (a) indicated.

proached as the density decreases. These correlations are much less obvious when the line-average density $n_{\mathrm{lin}}$ is considered. When the separatrix density was held constant above the H–L threshold (Fig. 2(b)) steady-state H-modes were obtained for the duration of the heating power pulse. The dashed horizontal lines, indicating the separatrix density for the L–H and H–L transitions respectively are identical on both these figures.

The importance of the separatrix density rather than edge electron temperature was confirmed by the experiment illustrated on Fig. 3, in which the H-mode was initiated during the ECRH heating plateau by a gas puff into the plasma chamber. Since ray tracing calculations have confirmed that the electron cyclotron absorption zone is not significantly shifted by the change in density, the gas puff, which raised the edge density, certainly lowered the edge electron temperature by ionization and equipartition losses. The edge ion temperature probably decreased due to dilution, but an increase due to improved energy equipartition with electrons cannot be ruled out.

## 4. Edge density dependence of ELM frequency

The ELM frequency depends sensitively on the edge density, as demonstrated on Fig. 4. The density was modulated in H-mode by gas puffs, and for each increase of separatrix density, the ELM repetition rate decreases. This experiment establishes a causality between separatrix density and ELM frequency. In addition, a doubling of the ELM has been observed when the helium content of the plasma is high. In the experimental traces presented in the following figures and discussed below, care has been taken that the separatrix densities and

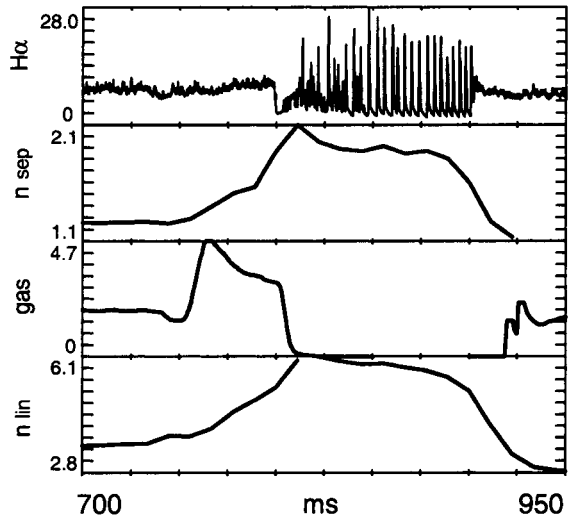


Fig. 3. H-mode obtained at constant heating power by neutral gas injection into the plasma chamber. The same quantities are plotted as in Fig. 2.

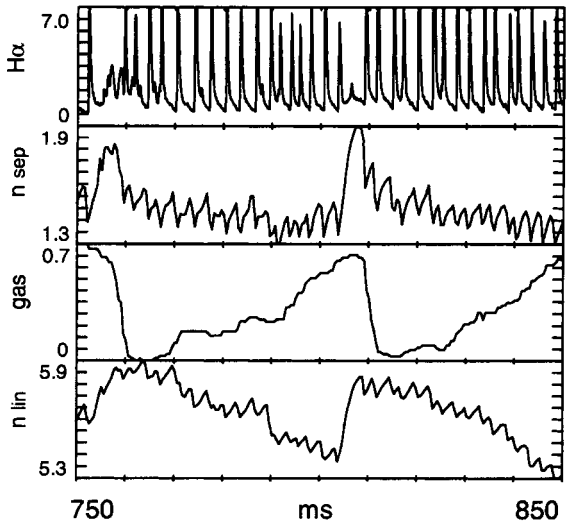


Fig. 4. Decrease of ELM repetition rate with increased separatrix density in density modulation experiment. The same quantities are plotted as in Figs. 2 and 3.

helium fractions (present from glow discharge cleaning and outgassing of the high heat load surfaces) were comparable for each series of experiments presented.

## 5. Threshold for the L–H transition

In Figs. 5 and 6, the input heating power at the transition has been plotted against line average and separatrix density respectively. These plots include both L–H transitions for ECRH with favorable $\nabla B$ drift, ECRH with unfavorable $\nabla B$ drift, and Lower Hybrid heating with favorable $\nabla B$ drift. For the H–L back transition, only points for ECRH with favorable $\nabla B$ drift and OH alone after ECRH turn-off are plotted.

The range of variation of total input power is quite limited, only a factor of two, because with increasing heating power, the ohmic input power falls by ~100 kW. For the ohmic heated cases, $-\mathrm{d}W/\mathrm{d}t$ provides sufficient power to also raise the net input power to the 400 kW range.

In terms of the line-average density (Fig. 5), the lower values of threshold power are consistent with the ITER H-mode power threshold scaling laws [3], which are expressed in terms of total heating power. The scaling law without elongation dependence (Eq. (1) of Ref. [3]: $P_{in} = 0.65 n^{0.93} B^{0.86} R^{2.15}$ [$10^{20}\mathrm{m}^{-3}$, T, m]) fits the results somewhat better than that with elongation dependence (Eq. (2) of Ref. [3]: $P_{in} = 0.42 n^{0.8} B^{0.9} R^{1.99} \kappa^{0.76}$). No significant hysteresis is obtained between L–H and H–L transitions (H–L transitions are joined with a dotted line on the figure), nor is there a significantly different power threshold for the two $\nabla B$ directions.

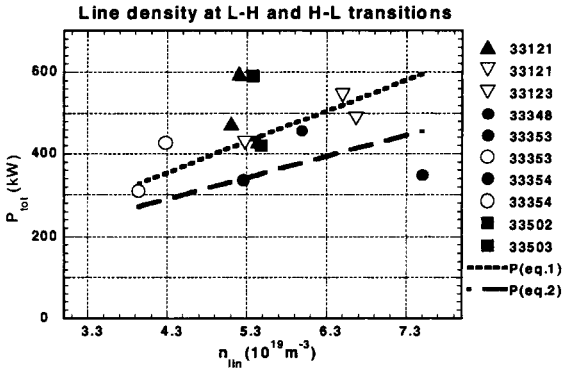


Fig. 5. Total input power vs. line average density at the L–H threshold. Filled symbols denote L–H transitions, open symbols H–L transitions. Ohmic-heated values are indicated by open circles, lower-hybrid heating by filled circles. All values except for the two filled squares are for $\nabla B$ drift towards the divertor. The ITER threshold power scaling laws are indicated for reference by thick lines, dotted without and dashed with elongation dependence.

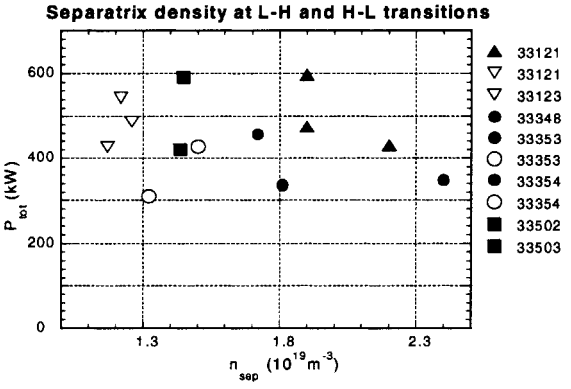


Fig. 6. Total input power vs. separatrix density at the L–H threshold. Filled symbols denote L–H transitions, open symbols H–L transitions. Ohmic-heated values are indicated by open circles, lower-hybrid heating by filled circles. All values except for the two filled squares are for $\nabla B$ drift towards the divertor. A clear hysteresis in separatrix density is observed.

In terms of the separatrix density (Fig. 6), there is a clear separation between the L–H and the H–L threshold, as expected from the time traces discussed in the preceding section. The L–H transition for the 'unfavorable' $\nabla B$ direction actually lies at lower values of separatrix density, comparable to those for the H–L transition with 'favorable' $\nabla B$.

## 6. Edge density fall-off length

Reflectometer measurements of the density gradient in the scrape-off layer give fall-off lengths at the midplane of 1.5–2.2 cm in L-mode with ECRH heating. In H-mode, 0.8–1.7 cm have been measured. The scrape-off length appears to increase with injected ECRH power, the lower values corresponding to 200–250 kW, the higher ones to 450–500 kW. For TdeV equilibria, 1 cm at the midplane corresponds to 6% of poloidal flux. The variations described in the following sections were carried out at 500 kW injected power, so that for the purpose of the discussion, we will take 10% of flux as one L-mode scrape-off length $\Delta_{\text{L-SOL}}$.

## 7. H-mode with reduced X-point baffle separation

The effect of reducing the separation between the separatrix and the divertor baffle (case B of Fig. 1) from 2.5 to 0.7 $\Delta_{\text{L-SOL}}$ (25–7% of flux) is illustrated on Fig. 7. As the distance is decreased to approximately $\Delta_{\text{L-SOL}}$, the time to H-mode transition increases somewhat, from ~15 to 19 ms [Fig. 7(a)], and is accompanied by a slight increase in ELM repetition rate [Fig. 7(b)]. Only at the smallest distance of 0.7 $\Delta_{\text{L-SOL}}$ is there an appreciable increase both in time to transition (50 ms) and in ELM frequency (~×2). Both indicate that the power threshold has increased as the separation was reduced. It should be pointed out that the final step of reducing the baffle separation resulted in a strong increase in helium contamination (present from glow-discharge cleaning), which has, in other runs, also been seen to increase the ELM frequency.

## 8. H-mode with reduced outboard separation

The effect of reducing the separation between the separatrix and an outboard limiter (case C of Fig. 1) to $\Delta_{\text{L-SOL}}$, (10% of flux) is illustrated on Fig. 8. The closest approach case (0.7 $\Delta_{\text{L-SOL}}$), for which an H-mode was also obtained, is not illustrated on the figure, because the very strong outgassing of helium from the carbon does not allow a direct comparison. Similarly to the previous section, the time to transition increases as the distance is reduced, from ~8 to 15 ms (Fig. 8(a)), and the ELM repetition rate increases by about 10–20% (Fig. 8(b)).

## 9. H-mode with reduced lower separation and variable lower triangularity

No systematic variation as for the two previous variations can be presented for the reduction of the lower gap (series D0, D1, and D2 of Fig. 1). Even though the distances, in either centimetres or scrape-off layers, were comparable for cases D1 and D2, no difficulty was encountered in establishing steady-state H-modes for geometry D1, whereas the same control pa-

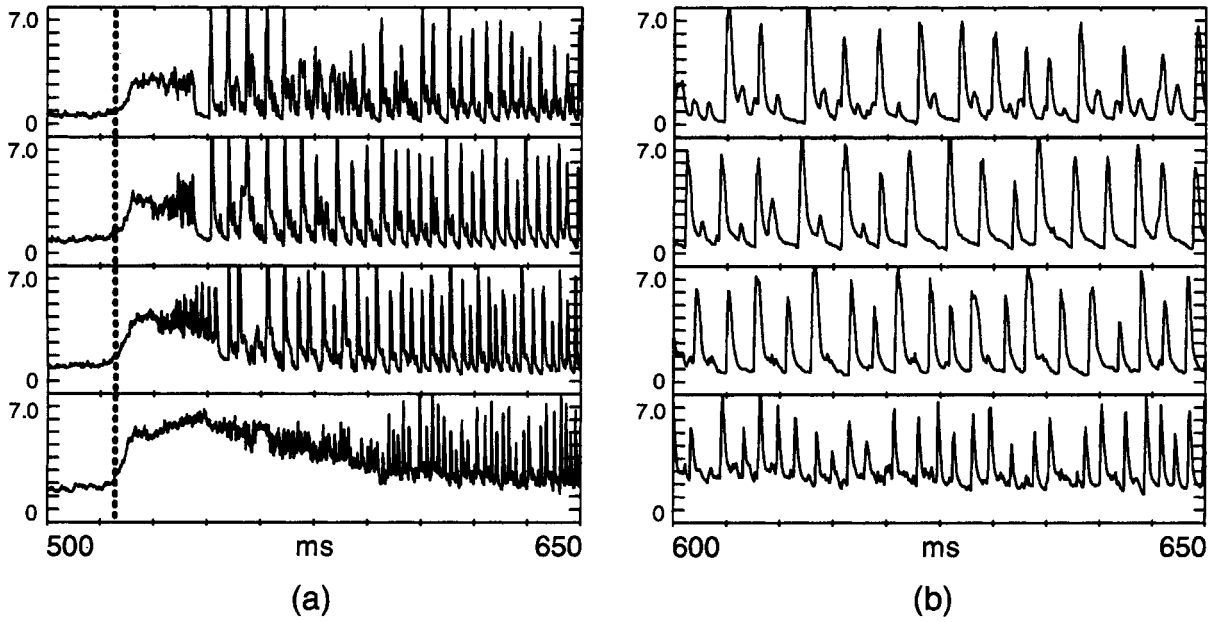


Fig. 7. Hα emission ($10^{19}$ photons/m$^2$/s) vs. time for, top to bottom, decreasing separatrix–divertor baffle gap. (a) H-mode onset; (b) steady-state ELMs.

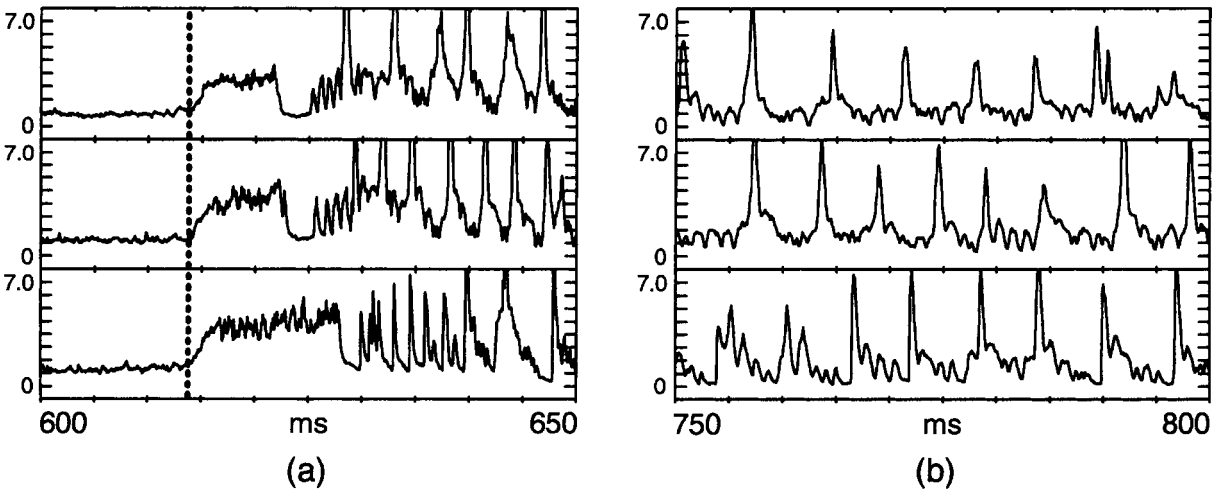


Fig. 8. Hα emission ($10^{19}$ photons/m$^2$/s) vs. time for, top to bottom, decreasing outboard separatrix–limiter gap. (a) H-mode onset; (b) steady-state ELMs.

rameters reproducibly produced L-modes in configuration D2. As far as geometry is concerned, the major difference between the two cases appears to be the lower triangularity, $\delta_{95}$, which was 0.14 for D1 and 0.2 for D2. The upper triangularity and elongation at the 95% flux surface are comparable. Transient H-modes were eventually obtained in configuration D2, but with appreciably higher gas puffing rates than necessary for configuration D1 or D0. The reason for the difference remains unclear.

## 10. Summary for H-modes with reduced gaps

On Fig. 9, the ratio of stored energy from diamagnetic measurements in H-mode to that in L-mode is

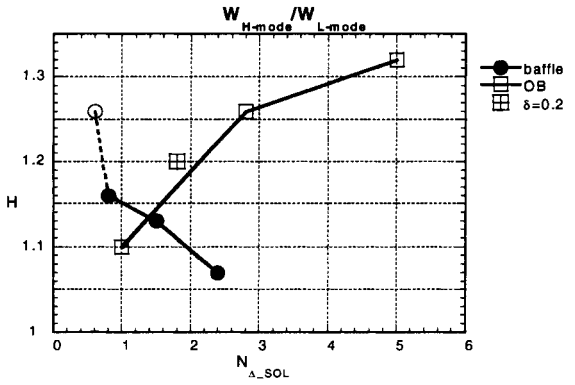


Fig. 9. Ratio of diamagnetic measurement in H-mode to that in L-mode plotted against gap width expressed in number of L-mode density scrape-off layers. Round symbols for separatrix – divertor baffle gap, square for decreasing outboard separatrix – limiter gap. The higher triangularity case is also indicated.

plotted for the gap variations and for the same shot series described above.

The abscissa is the gap width normalised to L-mode density scrape-off layers $\Delta_{\text{L-SOL}}$. As the outboard separation is reduced, the confinement appears to degrade. The H-mode with increased lower triangularity appears comparable in confinement with the normal case. However, an improvement in H-mode confinement over L-mode is observed as the separatrix to divertor baffle distance is reduced (as discussed above, the smallest separation had a much higher He content, and is therefore only joined with a dashed line).

## 11. Conclusion

Steady-state H-modes in type III ELM regime have been produced on TdeV with electron cyclotron and lower hybrid heating. The input power for L–H transition is consistent with the ITER threshold power scaling laws. In terms of line-average density, no hysteresis is observed between L–H and H–L transitions.

The L–H transition in TdeV is extremely sensitive to the separatrix density, which manifests itself as a threshold density below which no L–H transitions were obtained with the available power. In terms of separatrix density, there is a clear hysteresis between L–H transitions, which occur at a higher value than H–L transitions for the same input power.

In contrast to the experiments reported in [4], when the separatrix density was controlled, H-modes were obtained with an outboard separatrix–limiter distance less than or of the order of one density scrape-off length. The confinement at the smallest distance was reduced by about 10%. Reduction of the separatrix–divertor baffle distance was reduced by about 10%. Reduction of the separatrix–divertor baffle distance in a similar fashion improved the H-mode confinement over a more open configuration.

## Acknowledgements

CCFM is supported by the Government of Canada, Hydro-Québec, and INRS.

## References

[1] H. Zohm, Plasma Phys. Contr. Fusion 38 (1996) 105.
[2] J.-L. Lachambre, M. Gagne, Rev. Sci. Instrum. 65 (1994) 3428.
[3] The ITER H-mode Threshold Database Working Group (pres. by J.A. Snipes), Proceedings of the 24th European Conference on Controlled Fusion and Plasma Physics, Berchtesgaden, 1997, Part III, European Physical Society, p. 961.
[4] N. Suzuki, et al., Proceedings of the 14th European Conference on Controlled Fusion and Plasma Physics, Madrid, 1987, Part I, European Physical Society, p. 217.